International Journal of Plasticity, Vol. 7, pp. 275–293, 1991
Printed in the U.S.A.

0749-6419/91 $3.00 + .00

EVOLUTION EQUATION FOR THE VOID VOLUME GROWTH RATE IN A VISCOPLASTIC-DAMAGE CONSTITUTIVE MODEL

J. EFTIS* and J. A. NEMES†

*George Washington University and †Naval Research Laboratory

Abstract—A mathematical model for the rate of growth of microvoids under mean tensile stress in dynamic processes is developed, which represents an extension of previous analysis of ductile void growth rates using the hollow sphere model. A viscoplastic material is assumed for which the isotropic hardening saturates as the strain progresses. The microvoid growth model is used as an internal damage variable in Perzyna's elasto-viscoplastic constitutive theory for solids experiencing ductile modes of material damage. Several features of the void growth model are illustrated for a copper material, having been taken from our application of the viscoplastic-damage constitutive theory to model shock-induced high strain-rate deformation and spall fracture in polycrystalline solids.

I. INTRODUCTION

In several recent papers (EFTIS *et al.* [1991]; NEMES *et al.* [1989 a,b,c]), a modified form of the viscoplastic-damage constitutive theory developed by PERZYNA [1986] has been used to model high strain-rate behavior and shock-wave induced spall fracture. The original constitutive model assumed linear isotropic hardening, which had to be replaced by a more realistic nonlinear hardening rule, one that saturates as the strain progresses. As a consequence of this modification the equations that serve to describe evolution of material damage, that is, the rate of void growth of the microvoid volume fraction, had to be rederived. Since the rederivation entails considerable calculation, only the final results of this analysis are shown in the references cited above.

This paper describes in detail the development of an approximate analytical expression for the rate of growth of microvoids embedded in a rate-dependent plastic material that admits nonlinear hardening. A material model of this kind would be appropriate for polycrystalline solids that experience ductile modes of degradation and fracture. The development of the mathematical model for the void growth shown here draws upon and extends the earlier work of CARROL & HOLT [1972], JOHNSON [1981], and PERZYNA [1986], which make effective use of the thick hollow sphere model to develop constitutive models that describe the mechanical behavior of solid materials having porosity.

In describing mechanical behavior of polycrystalline materials for ordinary engineering applications, the presence of microvoids within the polycrystalline structure is not significant and is justifiably ignored. However in circumstances where material degradation occurs, either because of high intensity shock loading or because of advanced deformation, the porosity of the material structure becomes an important factor in attempting to describe the response of the material. Microvoids in polycrystalline metals can range from 10^{-2}–10^{-5} cm, with an average density of the order of 10^6 per cm^3, and an initial void volume fraction between 10^{-3}–10^{-4}. In the sequel when referring to structural metals as "porous solids," it should be borne in mind that our discussion is about materials that have initial porosities that are at least two orders of magnitude

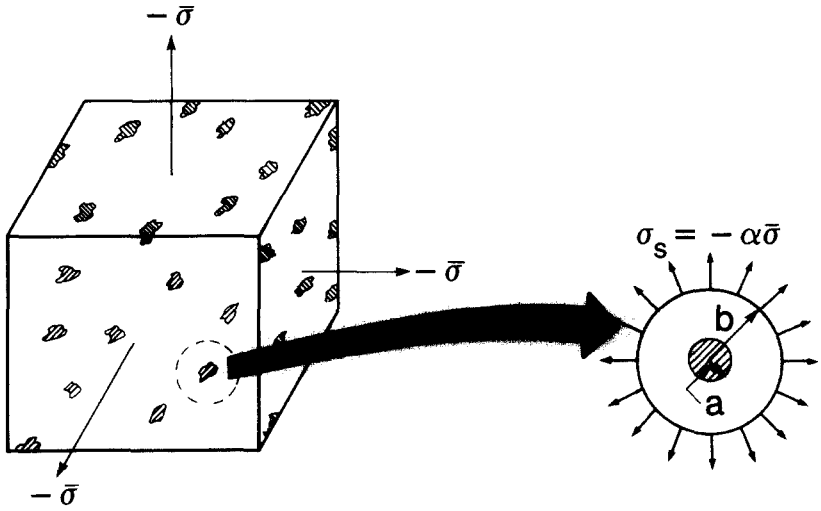

Fig. 1. Porous solid subjected to hydrostatic tension with idealized spherical microvoid.

smaller than the porosities of materials of geologic origin, or of materials encountered in powder metallurgy.

Microvoids in polycrystalline materials have arbitrary size and shape and are randomly distributed, thereby allowing the porous solid to be treated as a statistically homogeneous material that is isotropic. In the analysis for growth of microvoids it will be assumed that the dilatational contribution to the growth far overshadows any distortional contribution, so that the void growth can be considered to be entirely spherical. Thermal effects will not be considered.

Such limitations are closely satisfied in spall fractures that are induced by high velocity plate impact where, owing to the very high tensile mean stresses[1] that are generated by the reflected plane waves, void growth is predominately spherical. Also because of the very high strain rates involved (10^4–10^6 $\sec^{-1}$) material deformation is virtually adiabatic.

II. HOLLOW-SPHERE MODEL

In the process of developing a model for the porous solid, consider an arbitrarily small cubical volume element containing a representative distribution of voids on the surfaces of which act a uniform tension, ($\bar{\sigma}$), equal in all directions (cf. Fig. 1). The internal gas pressure within the voids can be ignored. With V as the total volume of the element, V_s and $V_v = V - V_s$ as the solid and void volume, respectively,

$$\xi = \frac{V_v}{V}, \quad \xi_0 \leq \xi < 1 \tag{1}$$

$$\alpha = \frac{V}{V_s} = \frac{1}{1-\xi}, \quad \alpha \geq \alpha_0 > 1 \tag{2}$$

[1]Mean stress levels of 1–100 kbars in materials with yield stress at 1–10 kbars.

define the void volume fraction and the void distention ratio. The zero subscripts designate initial values. Assuming that for a random distribution of void sizes and shapes the ratio of solid surface area to total surface area for each face of the volume element equals the ratio of the solid volume to the total volume, then it follows from mechanical equilibrium that

$$\sigma_s = -\frac{1}{1-\xi}\,\bar{\sigma} = -\alpha\bar{\sigma} \tag{3}$$

is the uniform tensile stress acting over the solid portion of each face of the element.

The hollow sphere model for the porous solid replaces each of the microvoids with a spherical microvoid surrounded by a thick spherical shell of solid material having inner radius (a) and outer radius (b), with a tensile radial stress $\sigma_s = -\alpha\bar{\sigma}$ applied along the outer spherical boundary (cf. Fig. 1). Corresponding to the spherical void geometry the void volume fraction and the void distention ratio have the values

$$\xi = \frac{\alpha - 1}{\alpha} = \left(\frac{a}{b}\right)^3 \tag{4}$$

and

$$\alpha = \frac{b^3}{b^3 - a^3}. \tag{5}$$

The main drawback of the model resides in the fact that in analyzing a porous solid volume element by a single isolated void surrounded by solid material, the effects of void interaction and coalescence that would enter into the analysis if the model were to consider all of the voids simultaneously are not accounted for. However the acceleration of void growth because of void interaction and coalescence can be introduced into the final expression for the void growth rate in the form of a postulated void interaction function (PERZYNA [1986]).

The radial loading produces spherically symmetric radial deformation of the solid material enclosing the void such that each point $P_0(r_0, \theta_0, \phi_0)$ of the reference configuration is displaced to the point $P(r, \theta, \phi)$ of the current deformed configuration whereby

$$\begin{aligned} r &= f(r_0, t) \\ \theta &= \theta_0 \\ \phi &= \phi_0, \end{aligned} \tag{6}$$

and the function f is continuous and differentiable. It has been shown that for materials having small initial porosities (JOHNSON [1981]), for example, $\xi_0 \sim 10^{-4} - 10^{-3}$, changes in the void distention as a result of the elastic and elastic-plastic phases of the deformation are very small (compared to the values expected at the latter stages of void growth). Consequently, a useful simplification can be introduced. For microvoid growth in materials having very small initial porosities, only the full plastic stage of the deformation around the void need be considered.

The condition that inelastic deformation of the solid spherical shell be isochoric requires that

$$f^2\left(\frac{\partial f}{\partial r_0}\right)_t = r_0^2, \tag{7}$$

which leads to the relation

$$r^3 = r_0^3 - B(t), \tag{8}$$

where $B(t)$ is an unspecified differentiable function related to the deformation of the surrounding material, and thus to the void volume growth. The spherically symmetric deformation produces acceleration components $a_r = \ddot{r}, a_\theta = a_\phi = 0$, with zero value for the shear stress components of the Cauchy stress tensor $\mathbf{T}$. The equations of motion for material points surrounding the void reduce to the single equation along the radial direction

$$\frac{\partial T_{rr}}{\partial r} + \frac{2}{r}(T_{rr} - T_{\theta\theta}) = \rho_s \ddot{r}, \tag{9}$$

where $T_{\theta\theta} = T_{\phi\phi}$, ρ_s is the density of the solid material and

$$\begin{aligned} T_{rr}(a,t) &= 0 \\ T_{rr}(b,t) &= -\alpha\bar{\sigma} \end{aligned} \tag{10}$$

are the boundary conditions at the spherical surfaces.

III. VOID VOLUME GROWTH RATE

Introducing the acceleration potential $\psi(r,t)$ such that

$$\ddot{r} = \frac{\partial \psi}{\partial r}, \tag{11}$$

then

$$\psi(r,t) = \frac{1}{3r}\ddot{B} + \frac{1}{18r^4}\dot{B}^2 \tag{12}$$

follows from eqns (11) and (8), and an integration of the equation of motion will give at each instant t

$$\rho_s[\psi(b,t) - \psi(a,t)] = -\alpha(t)\bar{\sigma} + 2\int_a^b \frac{1}{r}(T_{rr} - T_{\theta\theta})\,dr. \tag{13}$$

Furthermore, it follows using relations (5) and (8) that

$$\begin{aligned} b^3 - a^3 &= b_0^3 - a_0^3 \\ B(t) &= a_0^3 \frac{(\alpha_0 - \alpha)}{(\alpha_0 - 1)} \leq 0 \\ \frac{B(t)}{a^3} &= \frac{(\alpha_0 - \alpha)}{(\alpha - 1)} \leq 0 \\ \frac{B(t)}{b^3} &= \frac{\alpha_0 - \alpha}{\alpha} \leq 0, \end{aligned} \tag{14}$$

where the inequalities shown apply only for void growth for which $\alpha \geq \alpha_0 > 1$. These relations allow representation of the left side of the integrated equation of motion in terms of velocity and acceleration of the void distention,

$$\tau Q(\ddot{\alpha}, \dot{\alpha}, \alpha) = -\alpha(t)\bar{\sigma} + 2\int_a^b \frac{1}{r}(T_{rr} - T_{\theta\theta})\, dr \tag{15}$$

with

$$Q(\ddot{\alpha}, \dot{\alpha}, \alpha) = -\ddot{\alpha}[(\alpha - 1)^{-1/3} - \alpha^{-1/3}] + \tfrac{1}{6}\dot{\alpha}^2[(\alpha - 1)^{-4/3} - \alpha^{-4/3}] \tag{16}$$

and

$$\tau = \frac{\rho_s a_0^2}{3(\alpha_0 - 1)^{2/3}}.$$

Radial deformation of the spherical shell produces the displacement components

$$\begin{aligned} u_r &= r - r_0 = r - [r^3 + B(t)]^{1/3} \\ u_\theta &= u_\phi = 0. \end{aligned} \tag{17}$$

The corresponding spherical strain components are (small strain approximation)

$$\begin{aligned} E_{rr} &= \frac{\partial u_r}{\partial r} = 1 - \left[1 + \frac{B(t)}{r^3}\right]^{-2/3} \\ E_{\theta\theta} &= E_{\phi\phi} = \frac{1}{r} u_r = 1 - \left[1 + \frac{B(t)}{r_3}\right]^{1/3} \\ E_{r\theta} &= E_{r\phi} = E_{\theta\phi} = 0. \end{aligned} \tag{18}$$

In their calculations for pore collapse relations using this model CARROL and HOLT [1972] assumed rate-independent perfectly plastic material surrounding the void having the yield condition

$$(J_2')^{1/2} = \left[\frac{1}{2}\,\mathrm{tr}(\mathbf{T}'\cdot\mathbf{T}')\right]^{1/2} = \frac{1}{\sqrt{3}}\,Y_0, \tag{19}$$

in which $\mathbf{T}' = \mathbf{T} - \frac{1}{3}(\mathrm{tr}\,\mathbf{T})\mathbf{1}$ is the stress deviator and Y_0 is the rate-independent yield stress. Subsequent generalization of the model by JOHNSON [1981] for void growth calculation introduced rate-dependence for the nonhardening plastic deformation by means of the yield condition

$$(J_2')^{1/2} = \kappa(\dot{\bar{\epsilon}}^p) = \frac{1}{\sqrt{3}}\,(Y_0 + \bar{\eta}\dot{\bar{\epsilon}}^p), \tag{20}$$

where $\dot{\bar{\epsilon}}^p$ is the equivalent plastic strain rate, $\bar{\eta}$ is a material microviscosity parameter and $\bar{\epsilon}^p$, the equivalent plastic strain, is defined in terms of the octahedral plastic strain γ^p

$$\bar{\epsilon}^p = \sqrt{2}\gamma^p = \frac{2}{3}\,[(E^p_{\theta\theta} - E^p_{rr})^2]^{1/2} = \frac{2}{3}\left(\frac{u_r}{r} - \frac{\partial u_r}{\partial r}\right). \tag{21}$$

The void growth model was further generalized by PERZYNA [1986], whereby

$$(J_2')^{1/2} = \kappa(\bar{\epsilon}^p, \dot{\bar{\epsilon}}^p) = \frac{1}{\sqrt{3}}\,(Y_0 + H\bar{\epsilon}^p + \bar{\eta}\dot{\bar{\epsilon}}^p). \tag{22}$$

For reasons that are discussed in the sections that follow, it was found necessary to replace the linear hardening assumption by a nonlinear hardening rule wherein the hardening increases at a decreasing rate as the strain progresses, that is, it saturates (NEMES *et al.* [1989a]). For this kind of isotropic hardening

$$(J_2')^{1/2} = \kappa(\bar{\epsilon}^p, \dot{\bar{\epsilon}}^p) = q + (\kappa_0 - q)e^{-\beta\bar{\epsilon}^p} + \bar{\eta}\dot{\bar{\epsilon}}^p, \tag{23}$$

where $\kappa_0 = (1/\sqrt{3})Y_0$ and q, β are viscoplastic material hardening parameters. With

$$(J_2')^{1/2} = \frac{1}{\sqrt{3}}\,(T_{rr} - T_{\theta\theta}), \tag{24}$$

the integro-differential eqn (15) for the void distension ratio becomes

$$\tau Q(\ddot{\alpha}, \dot{\alpha}, \alpha) = -\alpha(t)\bar{\sigma} + 2\sqrt{3}\left\{\int_a^b \left(\frac{q}{r} + \frac{(\kappa_0 - q)}{r}\,e^{-\beta\bar{\epsilon}^p} + \bar{\eta}\,\frac{\dot{\bar{\epsilon}}^p}{r}\right)dr\right\}, \tag{25}$$

with

$$\bar{\epsilon}^p = -\frac{2}{3}\,\frac{B(t)}{r^3}\left(1 + \frac{B(t)}{r^3}\right)^{-2/3} \tag{26}$$

and

$$\frac{\dot{\bar{\epsilon}}^p}{r} = -\frac{2}{9}\,\frac{\dot{B}(t)}{r^4}\left[2\left(1 + \frac{B(t)}{r^3}\right)^{-5/3} + \left(1 + \frac{B(t)}{r^3}\right)^{-2/3}\right], \tag{27}$$

which follow from (18) and (21). Because of the smallness of the radial displacement at the microscale, the ratio $(r_0/r)^3 \approx 1$, which multiplies the right side of (27), is not shown.

Making use of (5), (14), and (27), integration of the first and third terms of the integrand of (25) gives

$$2\sqrt{3}\int_a^b \frac{1}{r}\,(q + \eta\dot{\bar{\epsilon}}^p)\,dr = \frac{2}{\sqrt{3}}\,q\ln\left(\frac{\alpha}{\alpha-1}\right) + \frac{2}{\sqrt{3}}\,\eta\,\frac{\dot{\alpha}}{\alpha(\alpha-1)}\,\bar{F}(\alpha,\alpha_0), \tag{28}$$

where

$$\bar{F}(\alpha,\alpha_0) = \alpha\left(\frac{\alpha-1}{\alpha_0-1}\right)^{2/3} - (\alpha-1)\left(\frac{\alpha}{\alpha_0}\right)^{2/3}, \quad \eta = \frac{2}{3}\,\bar{\eta}. \tag{29}$$

The remaining term of the integrand of (25) has the nonelementary integral form

$$2\sqrt{3}(\kappa_0 - q)\int_a^b \frac{1}{r}\,e^{-\beta\bar{\epsilon}^p}\,dr = \frac{2}{\sqrt{3}}\,(\kappa_0 - q)\int_{c_1}^{c_2} \frac{1}{z}\,e^{-c_3 z(1+z)^{-2/3}}\,dz, \tag{30}$$

where for any fixed value of t

$$z \equiv \frac{B(t)}{r^3}, \quad c_1 \equiv \frac{B(t)}{b^3}, \quad c_2 \equiv \frac{B(t)}{a^3}, \quad c_3 \equiv -\frac{2}{3}\,\beta, \quad \beta > 0, \tag{31}$$

and $-1 < c_2 < c_1 < 0$. For all points of the open interval $(-1,0)$ containing the closed interval $I = [c_2, c_1]$ the function $f(z) = \exp[-c_3 z(1+z)^{-2/3}]$ is differentiable and therefore continuous, with limit values $f(0) = 1$ and $f(-1) = 0$. Furthermore,

$$\frac{df(z)}{dz} = \exp[-c_3 z(1+z)^{-2/3}]\,(1+z)^{-2/3}\left[1 - \frac{2}{3}\,\frac{z}{(1+z)}\right] > 0 \quad \text{for } -1 < z < 0. \tag{32}$$

Thus $f(z)$ is a monotonically increasing function over the open interval $(-1,0) \supset I$. With $g(z) = 1/z$ continuous and bound over I, where $g(z) < 0$ for all $z \in I$, it follows by means of a mean value theorem for integrals (MILLER [1957]) that

$$\int_{c_1}^{c_2} \frac{1}{z}\,e^{-c_3 z(1+z)^{-2/3}}\,dz = e^{-c_3 z_0(1+z_0)^{-2/3}}\int_{c_1}^{c_2} \frac{1}{z}\,dz = 3\ln\left(\frac{b}{a}\right) f(z_0) \tag{33}$$

for some point $z_0 \in I$. Since $f(z)$ is monotonic it has a greatest lower bound value at $z = c_2$ and a least upper bound value at $z = c_1$. Therefore

$$3\ln\left(\frac{b}{a}\right) f(c_2) \le 3\ln\left(\frac{b}{a}\right) f(z_0) \le 3\ln\left(\frac{b}{a}\right) f(c_1), \tag{34}$$

and a good approximation for the value of the integral can be represented by the mean value of the upper and lower bound values

$$\int_{c_1}^{c_2} \frac{1}{z}\, e^{-c_3 z(1+z)^{-2/3}}\, dz \cong \frac{3}{2} \ln\left(\frac{b}{a}\right) [e^{-c_3 c_2 (1+c_2)^{-2/3}} + e^{-c_3 c_1 (1+c_1)^{-2/3}}]. \tag{35}$$

Substituting from (30), (31), (35), and (14) gives

$$2\sqrt{3}(\kappa_0 - q) \int_a^b \frac{1}{r}\, e^{-\beta \bar{\epsilon}^p}\, dr \cong \frac{1}{\sqrt{3}} (\kappa_0 - q) \ln\left(\frac{\alpha}{\alpha - 1}\right) \bar{F}_1(\alpha, \alpha_0), \tag{36}$$

where

$$\bar{F}_1(\alpha, \alpha_0) = \exp\left[\frac{2}{3}\beta\left(\frac{\alpha_0 - \alpha}{\alpha - 1}\right)\left(\frac{\alpha_0 - 1}{\alpha - 1}\right)^{-2/3}\right] + \exp\left[\frac{2}{3}\beta\left(\frac{\alpha_0 - \alpha}{\alpha}\right)\left(\frac{\alpha_0}{\alpha}\right)^{-2/3}\right]. \tag{37}$$

The integral results from (28) and (36) transform (25) into the following nonlinear second-order differential equation for the microvoid distention

$$\tau Q(\ddot{\alpha}, \dot{\alpha}, \alpha) - \frac{2}{\sqrt{3}} \eta \bar{F}(\alpha, \alpha_0) \frac{\dot{\alpha}}{\alpha(\alpha - 1)} - \frac{1}{\sqrt{3}} \{2q + (\kappa_0 - q)\bar{F}_1(\alpha, \alpha_0)\} \ln\left(\frac{\alpha}{\alpha - 1}\right) = -\alpha \bar{\sigma}. \tag{38}$$

The first term on the left side is the inertial resistance to void growth, and through τ is proportional to the density of the material surrounding the voids. The second and third terms represent the viscous and the nonlinear hardening resistances to the growth of microvoids.

In the limit as the rate of void distention approaches zero, it follows from (38) that

$$\lim_{(\ddot{\alpha}, \dot{\alpha}) \to 0} (-\alpha \bar{\sigma}) = -\frac{1}{\sqrt{3}} \{2q + (\kappa_0 - q)\bar{F}_1(\alpha, \alpha_0)\} \ln\left(\frac{\alpha}{\alpha - 1}\right) \equiv -\alpha \bar{\sigma}_G, \tag{39}$$

which represents the threshold hydrostatic tensile stress for void growth, with magnitude

$$|\bar{\sigma}_G| = \frac{1}{\sqrt{3}} \frac{1}{\alpha} \ln\left(\frac{\alpha}{\alpha - 1}\right) \{2q + (\kappa_0 - q)\bar{F}_1(\alpha, \alpha_0)\}. \tag{40}$$

The differential equation for the void distention rate therefore becomes

$$\tau Q(\ddot{\alpha}, \dot{\alpha}, \alpha) - \frac{2}{\sqrt{3}} \eta \bar{F}(\alpha, \alpha_0) \frac{\dot{\alpha}}{\alpha(\alpha - 1)} = -\alpha(\bar{\sigma} - \bar{\sigma}_G). \tag{41}$$

For polycrystalline materials the initial sizes of the microvoids are very small. The parameter τ, which is proportional to the microvoid dimension a_0^2 (cf. $(16)_2$), can therefore have very small values, suggesting that the void growth is dominated by viscous plastic deformation rather than by inertial effects. This has been demonstrated by JOHNSON [1981], who has shown that the inertial term in (41) can be many orders of magni-

tude smaller than the viscous contribution. Equation (41) can accordingly be simplified to the following expression for the microvoid growth rate

$$\frac{2}{\sqrt{3}}\eta\bar{F}(\alpha,\alpha_0)\frac{\dot{\alpha}}{\alpha(\alpha-1)}=\alpha(\bar{\sigma}-\bar{\sigma}_G). \tag{42}$$

Before applying this expression as part of a macroscopic description of the viscoplastic behavior of a solid that experiences damage in the form of void growth, several modifications need to be introduced. The uniform hydrostatic stress $\bar{\sigma}$ applied to the surface of a microvolume element with voids is now, from the macroscopic point of view, to be interpreted as the mean stress $\sigma = (1/3)\,\mathrm{tr}\,\mathbf{T}$ at each material point of the porous solid. To ensure nonnegative values for the void growth rate, the stress difference at the microscale, $(\bar{\sigma}-\bar{\sigma}_G)$, is replaced by the absolute value of the stress difference, $|\sigma-\sigma_G|$, at each material point of the porous body. It will be recalled that the analysis leading to (42), having employed an isolated hollow sphere model, takes no account of the void intereaction effects which tend to enhance the void growth rate. This process may be simulated by introduction of a positive valued material void interaction function, $g(\xi)$, (PERZYNA [1986]) in the manner shown below. With these modifications and with application of the transformation relation (4) to expressions (29), (37), (40), and (42), the equations describing the rate of growth of the void volume fraction can be summarized as follows

$$\dot{\xi}=\frac{1}{\eta}g(\xi)F(\xi,\xi_0)|\sigma-\sigma_G|,\quad \sigma<\sigma_G, \tag{43}$$

where

$$F(\xi,\xi_0)=\frac{\sqrt{3}}{2}\xi\left(\frac{1-\xi}{1-\xi_0}\right)^{2/3}\left[\left(\frac{\xi}{\xi_0}\right)^{2/3}-\xi\right]^{-1} \tag{44}$$

$$\sigma_G=-k_1\frac{1}{\sqrt{3}}(1-\xi)\ln\left(\frac{1}{\xi}\right)[2q+(\kappa_0-q)F_1(\xi,\xi_0)] \tag{45}$$

and

$$\begin{aligned}F_1(\xi,\xi_0)=&\exp\left[\frac{2}{3}\beta\frac{(\xi_0-\xi)}{\xi(1-\xi_0)}\left(\frac{1-\xi}{1-\xi_0}\right)^{-2/3}\left(\frac{\xi_0}{\xi}\right)^{-2/3}\right]\\&+\exp\left[\frac{2}{3}\beta\frac{(\xi_0-\xi)}{(1-\xi_0)}\left(\frac{1-\xi}{1-\xi_0}\right)^{-2/3}\right].\end{aligned} \tag{46}$$

We note that the minus sign in (45) signifies a tensile void growth threshold stress, while the constant k_1 represents a void interaction material parameter.

The material parameters and the material function appearing in these expressions can be determined from mechanical tests and from metallurgical data obtained at the temperature of interest (cf. NEMES *et al.* [1989a,c]). For example, a procedure for determination of the material function $g(\xi)$ can be based upon observations of microvoid growth data obtained from spall fracture tests. An illustration of this is discussed in Section V.

Finally, it should be noted that the microvoid growth rate equation (43), which does not include the inertial contribution to the void growth, is nevertheless used in formulating a viscoplastic-damage constitutive model for dynamical circumstances, and will be inserted into field equations that include the inertia term. Thus the simplification that has been introduced by writing (42) assumes, in effect, that the viscoplastic deformation dominates the microvoid growth process even though points of the deforming material body may be experiencing acceleration.

IV. CONSTITUTIVE MODEL FOR THE SOLID WITH MICROVOIDS

The mechanical behavior of a solid with microvoids includes elastic (recoverable) and inelastic (nonrecoverable and rate-dependent) components. Because of the presence of voids the elastic properties of the material are assumed to degrade with void growth according to the model proposed by MACKENZIE [1950], where the elastic shear and bulk moduli are determined by the relations

$$\bar{\mu} = \mu(1-\xi)\left(1 - \frac{6K + 12\mu}{9K + 8\mu}\,\xi\right)$$
$$\bar{K} = \frac{4\mu K(1-\xi)}{4\mu + 3K\xi}. \tag{47}$$

K, μ are the values of the bulk and shear moduli for the solid without voids (actually an idealization for polycrystalline materials that have some degree of porosity, although small, with typical average initial void volume fraction ξ_0 of the order 10^{-3}–10^{-4}). The Poisson ratio for the voided solid has the value

$$\bar{\nu} = \frac{1}{2}\,\frac{3\bar{K} - 2\bar{\mu}}{3\bar{K} + \bar{\mu}}. \tag{48}$$

The rate of deformation is the sum of the elastic and inelastic rates

$$\mathbf{D} = \mathbf{D}^e + \mathbf{D}^p. \tag{49}$$

Considering small elastic strains, the elastic rate of deformation has the form

$$\mathbf{D}^e = \frac{1}{2\bar{\mu}}\left[\mathring{\mathbf{T}} - \frac{\bar{\nu}}{1+\bar{\nu}}\,(\operatorname{tr}\mathring{\mathbf{T}})\mathbf{1}\right]. \tag{50}$$

$\mathring{\mathbf{T}}$ is the corotational (Jaumann) time rate of the Cauchy stress tensor $\mathbf{T}$.

The inelastic rate of deformation is determined by the viscoplastic constitutive model proposed by PERZYNA [1986] for dynamic fracture of ductile solids.

$$\mathbf{D}^p = \frac{\gamma}{\phi}\,\Phi(\hat{F})\,\frac{\partial f}{\partial \mathbf{T}} \qquad \text{for } \hat{F} > 0,$$
$$\mathbf{D}^p = 0 \qquad\qquad\qquad\quad \text{for } \hat{F} \le 0, \tag{51}$$

where Φ is a material functional of the yield function

$$\hat{F} = \hat{F}(\mathbf{T}, \epsilon^p, \xi) = \frac{f(J_1, J_2', \xi)}{\kappa(\epsilon^p, \xi)} - 1, \tag{52}$$

$\gamma = \gamma_0/\kappa_0$, κ_0 is related to the quasistatic yield stress while γ_0 is a macroscopic material viscosity parameter. The function ϕ is a rate of deformation control function that has as its argument the ratio of invariants $(I_2/I_2^s - 1)$, and is defined such that $\phi(0) = 0$ and $\phi(\ldots) \equiv 0$ for $(I_2/I_2^s < 1)$. I_2 is the invariant

$$\begin{aligned} I_2 &= \| (\mathrm{II}_{\mathbf{D}})^{1/2} \| \\ \mathrm{II}_{\mathbf{D}} &= \tfrac{1}{2}[(\mathrm{tr}\,\mathbf{D})^2 - \mathrm{tr}(\mathbf{D}\cdot\mathbf{D})], \end{aligned} \tag{53}$$

and I_2^s is the value of I_2 at the quasistatic rate of deformation.[2]

Because of the plastic dilatation by void growth, the yield function has both deviatoric and dilatational components (cf. SHIMA & OYANE [1976]; HANCOCK [1983]; DORAIVELU *et al.* [1984])

$$f(J_1, J_2', \xi) = J_2' + n\xi J_1^2, \tag{54}$$

where the stress invariants

$$\begin{aligned} J_1 &= I_{\mathbf{T}} = \mathrm{tr}\,\mathbf{T} \\ J_2' &= -\mathrm{II}_{\mathbf{T}} = \tfrac{1}{2}\mathrm{tr}(\mathbf{T}'\cdot\mathbf{T}'). \end{aligned} \tag{55}$$

The coefficient n is a material parameter that weights the effect of the void induced dilatation. The function $\kappa(\epsilon^p, \xi)$ describes the isotropic material hardening because of the plastic deformation, and the softening because of the void growth. The form originally proposed by PERZYNA [1986]

$$\kappa(\epsilon^p, \xi) = [\kappa_0 + H\epsilon^p]^2[1 - n_1\xi^{1/2}]^2 \tag{56}$$

assumes the linear hardening form $(\kappa_0 + H\epsilon^p)$ (cf. Section III), where H is a hardening parameter and ϵ^p is the plastic strain invariant defined by the relation

$$\epsilon^p = \int_0^t \dot{\epsilon}^p\, dt' = \int_0^t \frac{2}{\sqrt{3}} \|(\mathrm{II}_{\mathbf{D}^p})^{1/2}\|\, dt'. \tag{57}$$

The material parameter n_1 is related to the void volume fraction at fracture and may be shown to have the value $n_1 = (\xi_F)^{-1/2}$ (PERZYNA [1986, 1984]).

During the course of progressive material degradation in polycrystalline materials, leading to material instability and fracture, metallographic observations have shown that the void volume fraction can increase by several orders of magnitude (e.g., $\xi_0 \sim 10^{-3} \rightarrow$

[2]The rate of deformation below which no significant rate effect of the inelastic material response can be observed by the usual means of laboratory testing.

$\xi_F \sim 10^{-1}$ as observed in spall fracture of copper (CURRAN *et al.* [1987])). At the microvoid scale this order of change of void volume can be associated with relatively large strain around and between the microvoids. In such circumstances a linear monotonically increasing hardening rule can predict intense hardening, leading to a situation where the void growth threshold mean stress becomes very large, thereby preventing further void growth and stress relaxation at the larger strains. This result is demonstrated in more detail in the following section. As mentioned in the previous section, to circumvent such predicted behavior the hardening rule (56) is replaced by the form (NEMES *et al.* [1989a])

$$\kappa(\epsilon^p, \xi) = [q + (\kappa_0 - q)e^{-\beta\epsilon^p}]^2[1 - n_1\xi^{1/2}]^2, \tag{58}$$

which allows for saturation of the hardening as the strain progresses, where q is the saturation stress and β a hardening material parameter.

The material functional Φ and the control function are assumed to have power forms. Thus, the constitutive equation for the rate of inelastic deformation (51) acquires the detailed form

$$\mathbf{D}^p = \frac{\gamma_0}{\left(\frac{I_2}{I_2^s} - 1\right)^m}\left[\frac{J_2' + n\xi J_1^2}{[q + (\kappa_0 - q)e^{-\beta\epsilon^p}]^2[1 - n_1\xi^{1/2}]^2} - 1\right]^{m_1}\frac{1}{\kappa_0}(2n\xi J_1\mathbf{1} + \mathbf{T}'), \tag{59}$$

in which m and m_1 are additional viscoplastic material parameters.

Void volume change in general in polycrystalline materials has been identified and characterized by three micromechanisms: diffusion of voids, nucleation of new voids, and growth of existing voids due to plastic deformation. The diffusional microprocesses are significant only at elevated temperatures, so that at nonelevated temperatures the void volume fraction rate of change will consist essentially of void nucleation and void growth

$$\dot{\xi} = (\dot{\xi})_n + (\dot{\xi})_g, \tag{60}$$

where $(\dot{\xi})_g$ is obtained from (43). The rate of void nucleation is modeled by the relation (cf. CURRAN *et al.* [1987]; SEAMAN *et al.* [1976]; PERZYNA [1986])

$$(\dot{\xi})_n = \frac{h(\xi)}{1 - \xi}\left[\exp\left(\frac{m_2|\sigma - \sigma_N|}{k\theta}\right) - 1\right], \quad \sigma < \sigma_N. \tag{61}$$

σ_N is the threshold mean stress for void nucleation, θ is the temperature, k is the Boltzmann constant, and m_2 is a material constant. The function $h(\xi)$, introduced by Perzyna, represents the effect of void interaction on the void nucleation process, and is analogous to the void growth interaction material function $g(\xi)$ appearing in (43). Thus, the value of the void volume fraction appearing in the constitutive relations (47) and (59) is determined from (60), or

$$\dot{\xi} = \frac{h(\xi)}{1 - \xi}\left[\exp\left(\frac{m_2|\sigma - \sigma_N|}{k\theta}\right) - 1\right] + \frac{1}{\eta}g(\xi)F(\xi, \xi_0)|\sigma - \sigma_G|, \tag{62}$$

with $F(\xi, \xi_0)$ and σ_G specified by expressions (44)–(46).

In view of several comparisons that are to be discussed in the following section, we note here that with a linear hardening assumption (cf. (22) and (56)), the void volume rate due to the void growth $(\dot{\xi})_g$ will also be determined by (43) and (44). However, the corresponding expression for the threshold mean stress will now have the form (PERZYNA [1986]):

$$\sigma_G = -k_1\left[\frac{2}{3}\kappa_0(1-\xi)\ln\left(\frac{1}{\xi}\right) + \frac{2}{3}H(1-\xi)F_2(\xi,\xi_0)\right], \tag{63}$$

with

$$F_2(\xi,\xi_0) = 3\left(\frac{1-\xi}{1-\xi_0}\right)^{1/3}\left[1-\left(\frac{\xi_0}{\xi}\right)^{1/3}\right]. \tag{64}$$

V. EXAMPLES OF APPLICATION TO OFHC COPPER

The viscoplastic-damage constitutive theory, outlined above, has been used to model high strain-rate deformation and plate impact induced spall fracture for OFHC copper at room temperature. The reduced constitutive equations appropriate for calculating uniaxial stress–strain, and stress–uniaxial strain, are given in the references cited at the outset of the Introduction. A discussion of how the material parameters were determined or chosen can also be found there.

The manner of variation of the void growth threshold stress with increase of porosity is shown in Fig. 2 with three different assumptions for the hardening; nonlinear (cf. eqn 58)), linear (cf. eqn (56)), and nonhardening ($H = 0$ in eqn (56)). These curves illustrate the simultaneous competition that takes place between the hardening of the material as deformation increases, and the softening that accompanies the void growth. At small void volume fraction (and small strain) the strain-hardening process is much more influential than the void softening. This relationship is reversed as the void growth progresses and the material degradation overwhelms the ability of the material to continue hardening. Linear hardening produces a peak value for the threshold stress approximately twice the value for the nonlinear hardening that saturates, occurring at a porosity that is approximately 30 times as great. In the case of no strain hardening the void growth threshold decreases progressively as the material softens immediately with the onset of void growth.

The linear hardening, which continually increases as the strain progresses, endows the material with an unrealistic excess of hardening. This effect is graphically demonstrated by Fig. 3, which shows calculated tensile stress versus uniaxial strain at strain rate 10^5 sec^{-1} for the three hardening assumptions. The linear hardening, as expected, gives the highest stress prior to onset of stress relaxation caused by the degradation of the material. Because of the higher void growth threshold stress and the fact that its value begins to decrease at a much larger void volume fraction, the predicted stress relaxation appears virtually to cease at a high stress level, rather than continuing on with further increase of strain as would be expected on physical grounds. At the larger strains and, correspondingly, at the larger void volume fractions, the closer proximity of the nonlinear hardening stress–strain curve to the curve with no hardening also appears to be more realistic.

The material interaction function $g(\xi)$ appearing in (43) serves to amplify the rate of void growth at the later stages of the void development, thereby simulating the effects

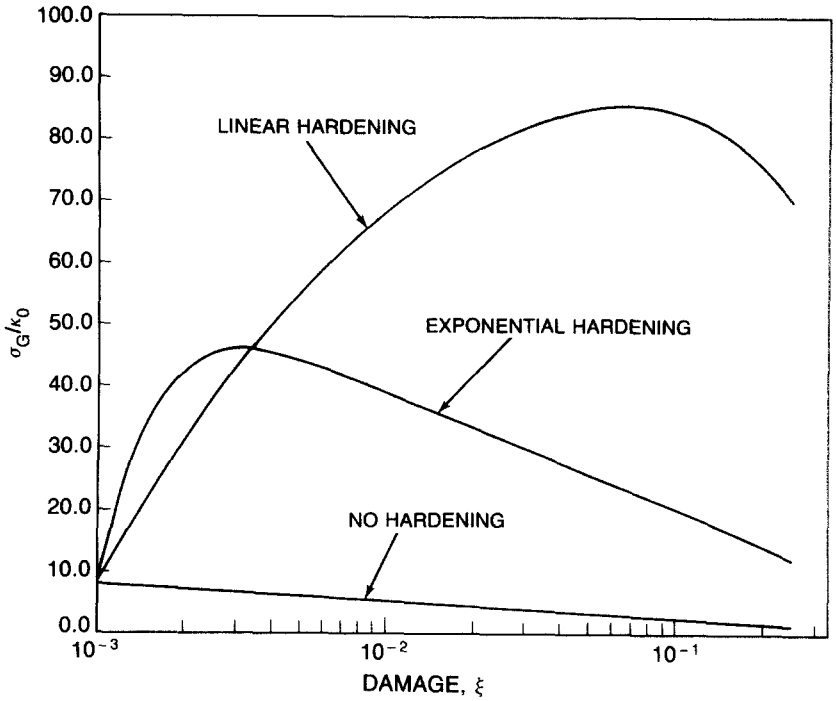

Fig. 2. Effect of hardening assumption on the void growth threshold stress.

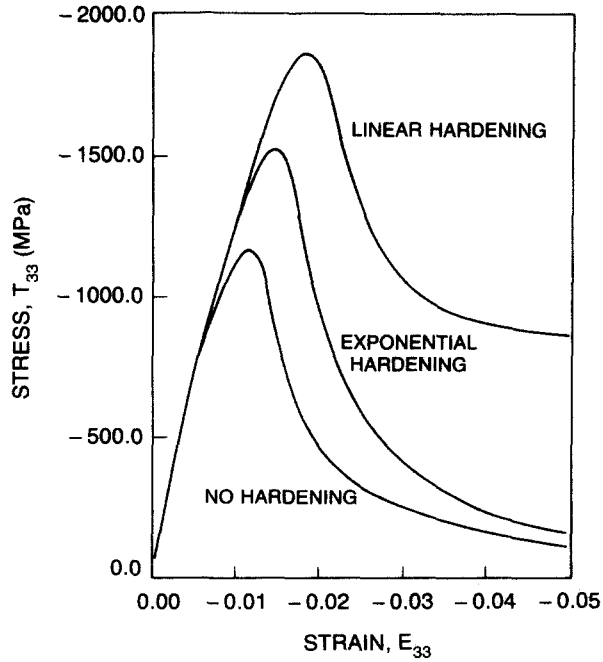

Fig. 3. Effect of hardening assumption on the stress versus uniaxial strain response at $D_{33} = -4 \times 10^5$ sec.$^{-1}$

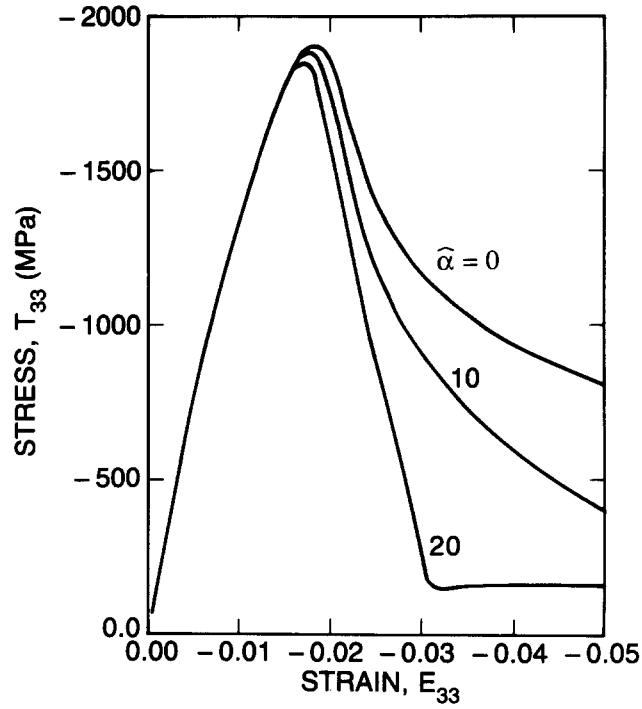

(a)

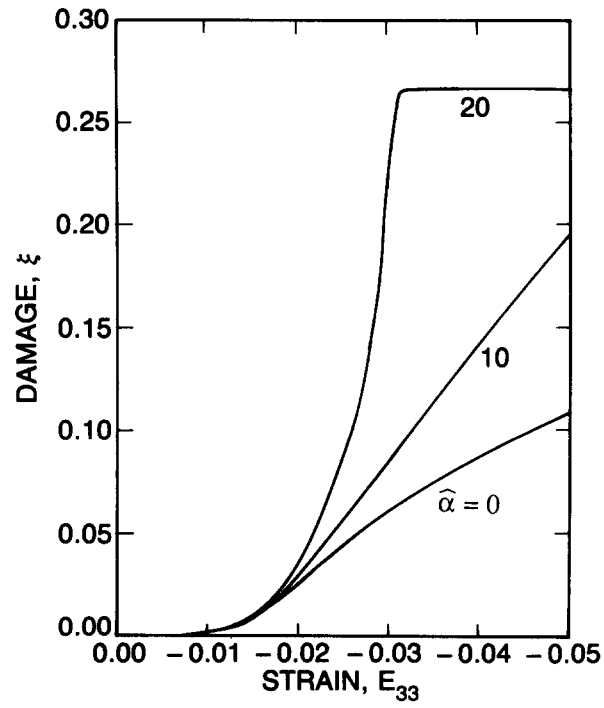

(b)

Fig. 4. Variation of $\hat{\alpha}$ for uniaxial strain at $D_{33} = -4 \times 10^5$ sec^{-1} (a) stress vs. strain, (b) damage vs. strain.

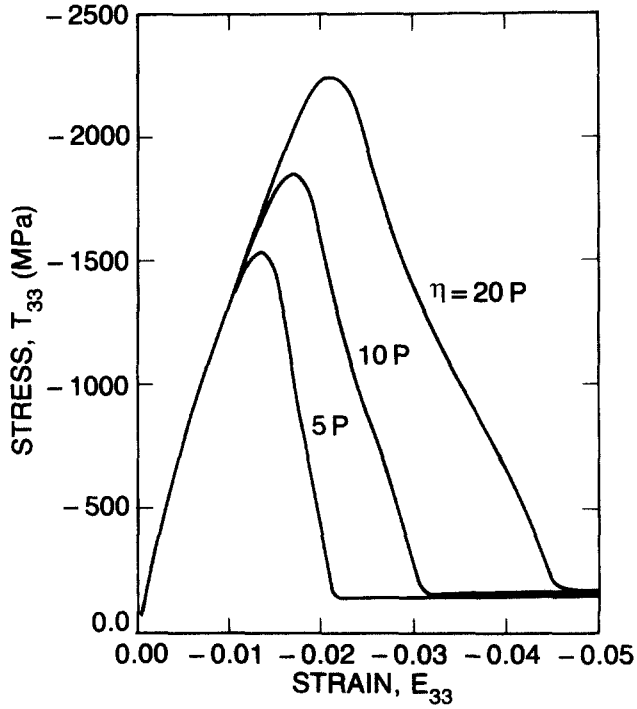

(a)

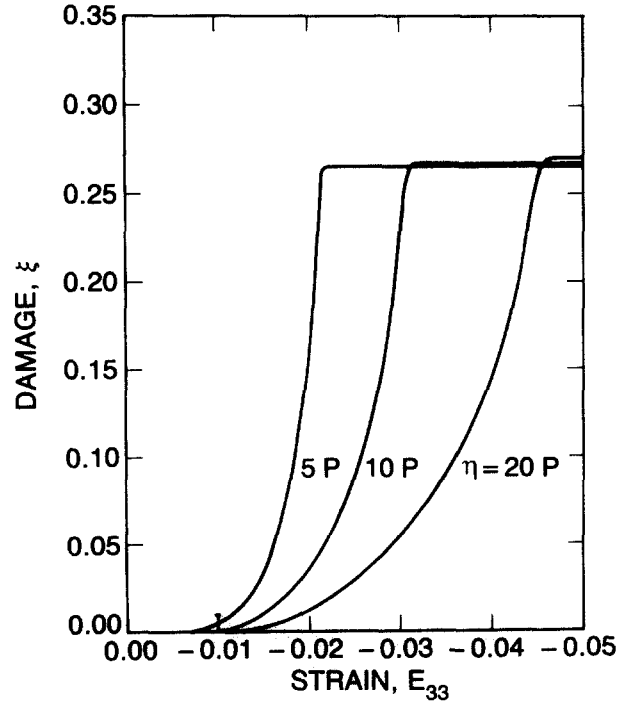

(b)

Fig. 5. Variation of η for uniaxial strain at $D_{33} = -4 \times 10^5$ sec^{-1} (a) stress vs. strain, (b) damage vs. strain.

of void interaction and coalescence. The function was chosen as an exponential of the void volume fraction, $g(\xi) = e^{\hat{\alpha}\xi}$ (where $\hat{\alpha}$ is a material parameter), based upon observed void volume distributions in spalled plates, and also because of its desirable characteristics at small and large values of ξ. The parameter value $\hat{\alpha} = 20$ gave good experimental data correlation for the spall fracture studies (NEMES [1989c]; EFTIS *et al.* [1989]). The relative effect of this material parameter on the stress–uniaxial strain response, and upon the rate of void growth with strain, is shown in Figs. 4a and 4b. The

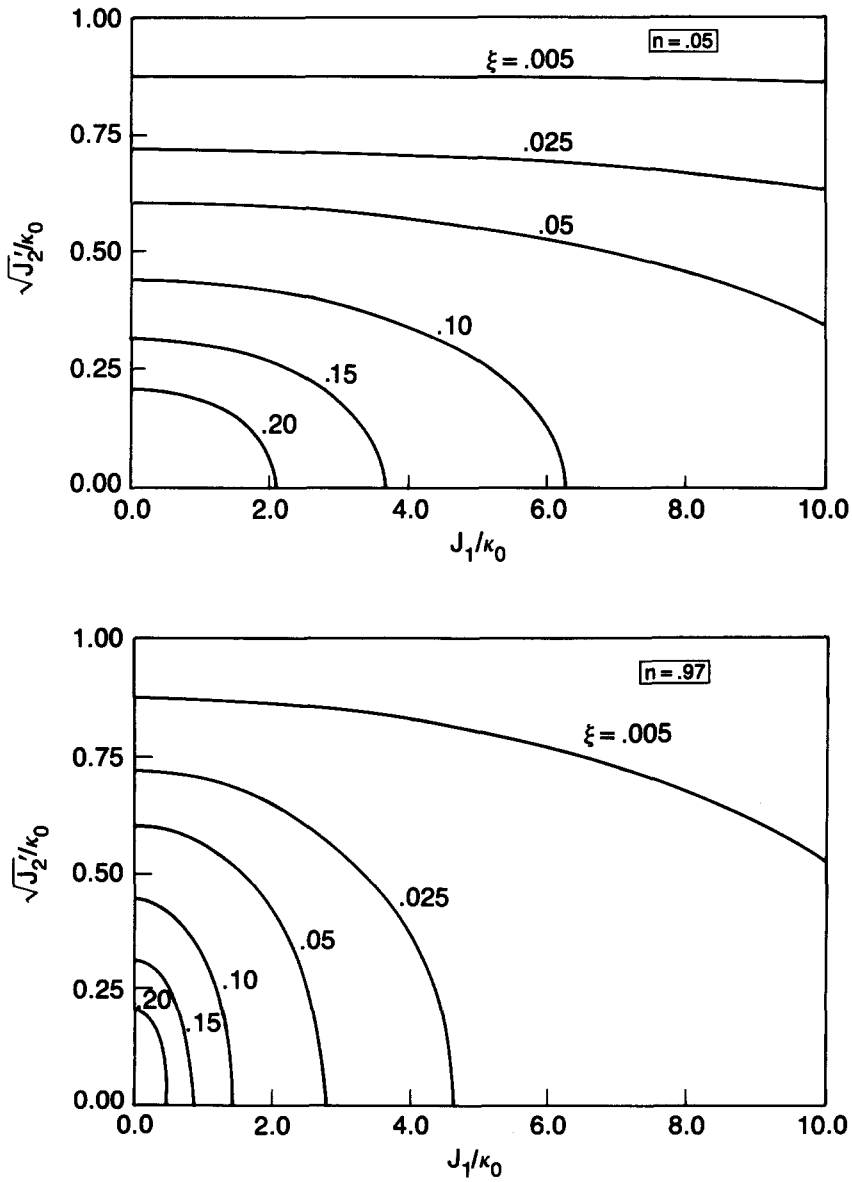

Fig. 6. Effect of varying porosity on the yield condition (a) $n = .05$, (b) $n = .97$.

curve for which $\hat{\alpha} = 0$, or $g(\xi) = 1$, corresponds to void growth with no void interaction on the void growth process. The peak tensile stress that occurs prior to softening is practically unchanged by the value for $\hat{\alpha}$ which, as seen from Fig. 4a, takes place at very small values of the void volume fraction where interaction effects would be expected to be negligible. The predicted behavior beyond the peak stress, however, is strongly affected by the value of this parameter, as one would expect since it is at the higher values of ξ that the interaction function $g(\xi)$ becomes significant. As the value of $\hat{\alpha}$ increases from $\hat{\alpha} = 0$ to $\hat{\alpha} = 10$, the rate of increase of damage increases considerably; however for $\hat{\alpha} = 20$ the void volume fraction increases dramatically for small changes in strain (cf. Fig. 4b), effectively simulating void coalescence behavior.

The relative effect of variation of the material microviscosity parameter η appearing in the void growth relation (42) on the macroscopic stress–strain behavior, and on the damage versus strain behavior, is indicated by Figs. 5a and 5b. The values of η shown bracket the value $\eta = 10$ P,[3] suggested by JOHNSON [1981], that was chosen for copper in the spall fracture study. It is rationalized by Johnson that this relatively low value for the microviscosity associated with the microvoid growth is due to substantial highly localized heating effects that develop at and around the plastically expanding micropore walls, creating local "hot spots" that can be at a substantial fraction of the melting temperature. (We note that published values for the viscosity for copper range from $\eta = 10^5$ P at room temperature to $\eta \approx 2 \times 10^{-2}$ P at melting temperature (CARROL *et al.* [1986]). As can be seen from the stress-uniaxial strain curves of Fig. 5a, and the damage–strain curves of Fig. 5b, the variation of η has strong influence on the predicted response. Larger values of η result in lower rates of increase of the porosity, and in higher peak stresses prior to the onset of softening. However, the strength of the viscosity is shown to have little effect on the rate of stress relaxation, and also upon the maximum void volume that is reached, which is close to the void volume fraction $\xi = 0.3$ observed for spallation of copper.

The effect that the void volume or porosity can have on the yield behavior of the material is illustrated in Figs. 6a and 6b, showing a plot of the yield function f, eqn (54), at different void volume fractions. As the porosity of the material increases and it softens, the effect of the mean stress (dilatation) on plastic yield becomes pronounced, and the combined stress state required for onset of yield decreases dramatically.

Acknowledgement – The authors wish to acknowledge the interest and encouragement extended by Dr. Phillip Randles and Dr. Robert Badaliance of the Mechanics of Materials Branch of the Naval Research Laboratory. The first author also expresses appreciation for the support made possible by the ASEE-NAVY Summer Faculty Research Program at NRL. The assistance of the reviewers in helping to clarify portions of the presentation is also gratefully acknowledged.

REFERENCES

1950 MACKENZIE, J.H., "The Elastic Constants of a Solid Containing Spherical Holes," Proc. Phys. Soc., **63B**, 2-11.
1957 MILLER, A.H., Advanced Real Calculus, Harper & Row, New York.
1972 CARROLL, M.M. and HOLT, A.C., "Static and Dynamic Pore-Collapse Relations for Ductile Solids," J. Appl. Phys., **43**. 1626–1636.
1976 SEAMEN, L., CURRAN, D.R., and SHOCKEY, D.A., "Computational Models for Ductile and Brittle Fracture," J. Appl. Phys., **47**, 4814–4826.
1976 SHIMA, S. and OYANE, M., "Plasticity Theory for Porous Solids," Int. J. Mech. Sci., **18**, 285–291.

[3] 1 Poise (P) = 1 dyne·sec/cm^2 = 10^{-7} MPa·sec.

1981 JOHNSON, J.N., "Dynamic Fracture and Spallation in Ductile Solids," J. Appl. Phys., **53**, 2812–2825.
1983 HANCOCK, J.W., "Plasticity of Porous Metals," in Yield, Flow and Fracture of Polycrystals, BAKER, T.N., (ed.), Applied Science, Essex, U.K.
1984 DORAIVELU, S.M., GEGEL, H.L., GUNASEKERA, J.S., MALAS, J.C., MORGAN, J.T., and THOMAS, J.F., JR., "A New Yield Function for Compressible P/M Materials," Int. J. Mech. Sci., **26**, 527–535.
1984 PERZYNA, P., "Constitutive Modeling of Dissipative Solids for Postcritical Behavior and Fracture," ASME J. Engng. Mater. Technol., **106**, 410–419.
1986 PERZYNA, P., "Internal State Variable Description of Dynamic Fracture of Ductile Solids," Int. J. Solids Structure, **22**, 797–818.
1986 CARROL, M.M., KIM, K.T., and NESTERENKO, V.F., The Effect of Temperature on Viscoplastic Pore Collapse," J. Appl. Phys., **59**, 1962–1967.
1987 CURRAN, D.R., SEAMEN, L., and SHOCKEY, D.A., "Dynamic Failure of Solids," Physics Reports, **147**, 253–388.
1989a NEMES, J.A., EFTIS, J., and RANDLES, P.W., "Viscoplastic Constitutive Modeling of High Strain-Rate Deformation, Material Damage, and Spall Fracture," ASME J. Appl. Mech., 57, 282–291.
1989b NEMES, J.A. and EFTIS, J., "Use of Viscoplastic Constitutive Theory for Simulating Spallation Thresholds," in Shock Waves in Condensed Matter—1989, SCHMIDT, S.C., JOHNSON, J.N., and DAVIDSON, L.W. (eds.), Elsevier Science, B.V., Amsterdam.
1989c NEMES, J.A., "A Viscoplastic Description of High Strain-Rate Deformation, Material Damage and Spall Fracture," Doctoral Dissertation, George Washington University, Washington, DC.
1991 EFTIS, J., NEMES, J.A., and RANDLES, P.W., "Viscoplastic Analysis of Plate-Impact Spallation," Int. J. Plasticity, **7**, 15–39.

Department of Civil, Mechanical and Environmental Engineering
George Washington University
Washington, DC 20052

(*Received* 10 *September* 1989; *in final revised form* 12 *February* 1990)